

Content from this work may be used under the terms of the CC BY 3.0 licence (© 2018). Any distribution of this work must maintain attribution to the author(s), title of the work, publisher, and DOI.

MULTIPACTOR DISCHARGE IN SUPERCONDUCTING ACCELERATING CH CAVITIES*

M. Gusarova^{1†}, D. Kiselev, MEPHI, National Research Nuclear University, 115409 Moscow, Russia
 M. Miski-Oglu, T. Kuerzeder, F. Dziuba, HIM Helmholtz Institute Mainz, 55099 Mainz, Germany
¹also Joint Institute for Nuclear Research, Dubna, Russia

Abstract

The results of numerical simulations of multipacting discharge in a superconducting accelerating Crossbar H-type (CH) cavity are presented in this paper. The localization of multipactor trajectories in the 15-gap 217 MHz superconducting (sc) CH cavity at various levels of accelerating voltage is considered.

INTRODUCTION

The goal of the ongoing UNILAC (UNIversal Linear ACcelerator) upgrade program at GSI is to provide high intensity heavy ion and proton beams [1-5] for the Facility of Antiproton and Ion Research at Darmstadt (FAIR) [6]. Due to the low duty factor requirements for FAIR injector operation, a use of the UNILAC for super heavy element (SHE) research at GSI will be strongly limited. A dedicated standalone superconducting (sc) continuous wave (cw) linac HELIAC (HElmholtz LInear ACcelerator) is assumed to meet the demands of the experimental program [7]. The first RF test of a sc CH cavity was performed at Goethe University Frankfurt in a vertical cryostat [8]. After final assembly of the helium vessel and further High Pressure Rinsing (HPR) the RF test in a horizontal cryostat [9] at GSI was carried out. Subsequently, in summer 2017 the cavity was successfully commissioned with beam [10] at GSI. During RF tests, the cavity was operated as a generator driven resonator directed by an RF control system. Fig. 1 shows the 3D model of the superconducting (sc) 15-gap CH cavity for the (cw) linac HELIAC.

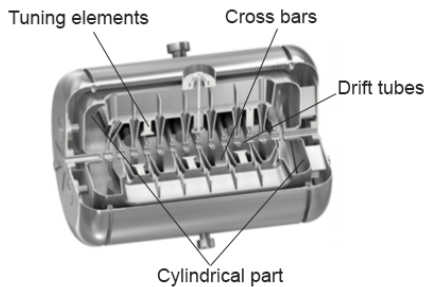


Figure 1: 3D model of the sc 217 MHz CH cavity.

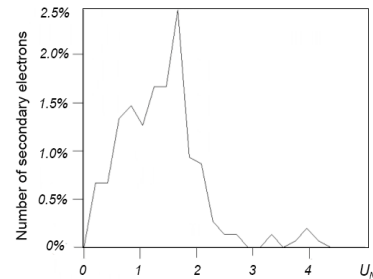
All multipacting barriers up to 4 MV/m could be permanently surmounted [8, 9], but during testing at low field levels stable and inevitable levels of a multipactor discharge were detected. This paper investigates the location and possible expansion of the multipactor discharge at different field values.

WIDE RANGE VOLTAGE SCAN

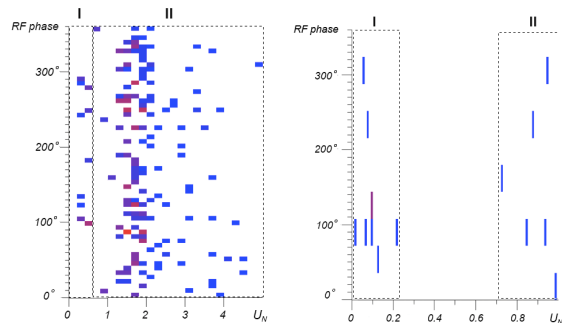
For the investigation of multipacting discharge effects the MultP-M code [11], developed at MEPHI, has been used. The electromagnetic field is exported from the CST studio [12]. The calculations have been carried out for a wide range of RF-voltage and RF-phase.

The voltage amplitudes U_N are normalized to the unit voltage value of $U = \int E_z dz = 2.8$ MV, integrated at 1 J stored energy inside the cavity, i.e $U_N = 1$ corresponds to $U = 2.8$ MV.

In order to identify the most dangerous multipacting levels, the simulations were performed with different steps of U_N : over a wide U_N range from 0 to 5 with the rough step width of 0.2 (RF phase step is 6°), in the range $U_N = 0 - 1$ with steps of 0.04 (RF phase step is 36°) and for $U_N = 0 - 0.01$ with steps of 0.0004 (RF phase step is 6°). The calculations take the RF-phase, at which an electron hit the surface, into account. Fig. 2(a) shows the number of surviving electrons versus the RF voltage. Here the electrons from all initial RF phases (but the same voltage level) are summed up. The calculation time was limited to 10 RF periods.



(a)



(b)

(c)

Figure 2: (a) Number of surviving electrons versus voltage level after 10 RF periods; (b) diagram RF phase / U_N

This is a preprint — the final version is published with IOP

* Work supported by FAIR-Russia Research Center (FRRC)

† MAGusarova@mephi.ru

for $U_N = 0 - 5$ with a step width of 0.2; (c) diagram RF phase / U_N for $U_N = 0 - 1$ with a step width of 0.04.

Fig. 2(b) shows the diagram RF phase / U_N . For each pair of RF phase and U_N , the code tracks the trajectories of 100 electrons randomly distributed over the structure. Cavity length is 0.8m. Each square in Fig. 2(b) and Fig. 2(c) corresponds to the voltage level and RF phase electron collision at which multipactor trajectories are detected. As soon as an electron with an energy for which Secondary Emission Yield $SEY > 1$ (used SEY for baked 300° Nb [13], $SEY > 1$ when the electron has an energy between 50 and 1500 eV) hits the wall for the first time, the counter function starts an account of trajectories. A secondary electron is generated and traced until either 10 RF periods are reached, or the number of hits with the surface reach a limit of impacts ($n=5$). For the calculation it is assumed, that the initial energy of the secondary electrons is zero and the direction of the emission is normal to the surface. The red colour denotes the regions with the largest number of surviving electrons, and the blue colour the less populated region. The graphs in Fig. 2 illustrate the existence of trajectories persisting more than 10 RF periods.

Two groups of trajectories could be recognized in Fig 2b: region I and II. The visual inspection of the corresponding electron trajectories, calculated at different voltage levels, shows at low voltage levels a concentration of the trajectories in the area of tuning elements and cross bars (region I Fig. 2b and Fig.2 c). Fig. 3 illustrates some examples of trajectories at $U_N = 0.042$ and $U_N = 0.208$. Red color indicates the trajectory of the primary electron, the blue of the first knocked out, the subsequent green.

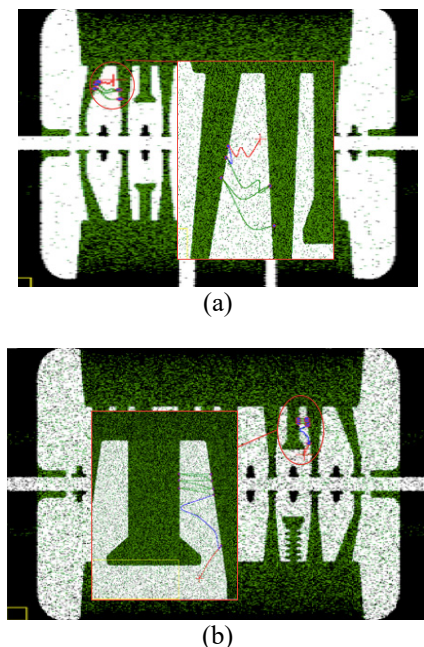


Figure 3: Example of multipactor trajectories at a low level voltage: (a) $U_N = 0.042$; (b) $U_N = 0.208$.

As shown in detailed study of the electron trajectories, in the range of U_N from 0.04 to 0.22, trajectories are

damped; corresponding to two point multipacting trajectories. Resonance conditions are absent.

At higher voltage levels (region II of Fig. 2b and Fig. 2c, $U_N > 0.7$), the trajectories are mainly concentrated on the cylindrical part of accelerating structure. An example of a trajectory at $U_N = 0.875, 1.173$ and 1.25 is shown in Fig. 4.

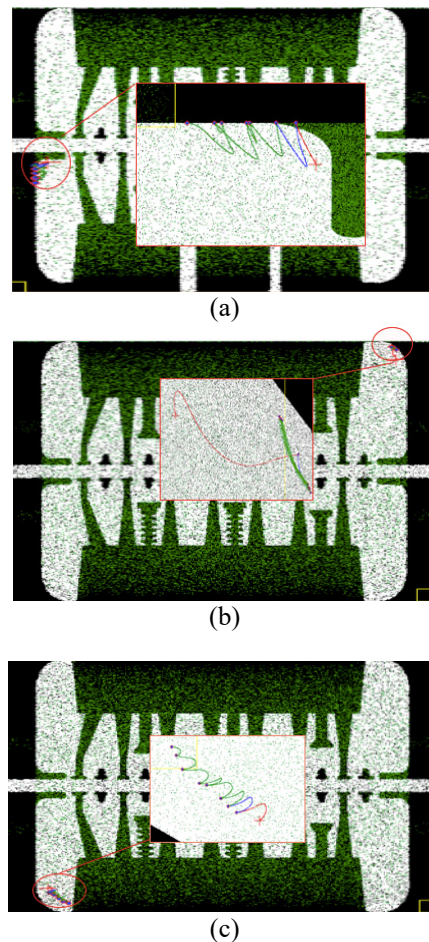


Figure 4: Example of multipactor trajectories at a different level voltage: (a) $U_N = 0.875$; (b) $U_N = 1.173$; (c) $U_N = 1.25$.

Two types of trajectories were identified: fast damped one-point multipactor trajectories (see Fig. 4a and Fig. 4c) and slowly damped two-point multipactor trajectories (see Fig. 4b). Along the trajectory an electron gains energy within the first RF periods (up to 200 -1200eV). The electrons on fast damped one-point multipactor trajectories within 3-10 RF periods lose their initial energy which drops to less than 20 eV. For slowly damped two-point multipactor trajectories the electron's energy drops down within 30-40 RF periods.

Figure 5 shows the number of secondary electrons as function of U_N for 50 and 100 RF periods. One can recognize, that slowly damped trajectories are mainly concentrated at low voltages ($U_N < 0.5$).

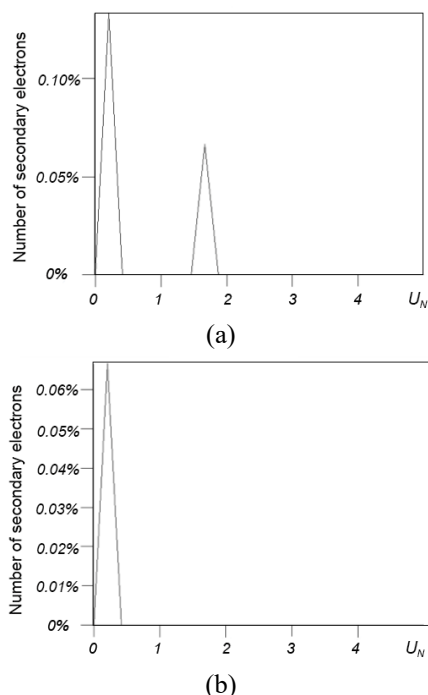


Figure 5: Number of surviving electrons versus the voltage level after 50 (a) and 100 (b) RF periods.

LOW VOLTAGE RANGE

The low voltage range was considered separately. The calculations have been performed for U_N in a range from 0 to 0.01 with steps of 0.0004. Fig. 6 shows the RF phase / U_N diagram, where no trajectory below $U_N < 0.003$ is found. Visual inspections of trajectories show, that they are localized between drift tubes. Fig. 7 shows exemplary trajectories at different low voltage levels. The trajectories are damped and correspond to two point multipacting trajectories. The trajectories are damped about from 10 to 40 RF periods but the electron can gain energy up to 250 – 450 eV close to the maximum of the SEY emission for Nb [13] which can be the cause of the difficult suppression of the multipactor at these levels.

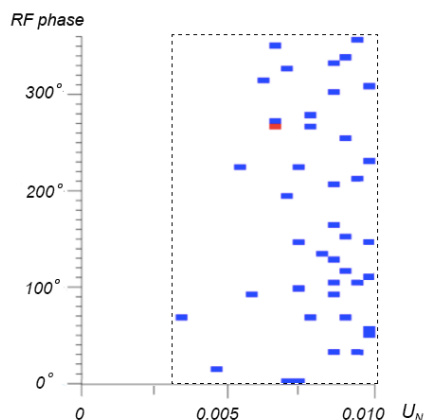


Figure 6: Diagram RF phase / U_N for $U_N = 0 - 0.01$ with step 0.0004.

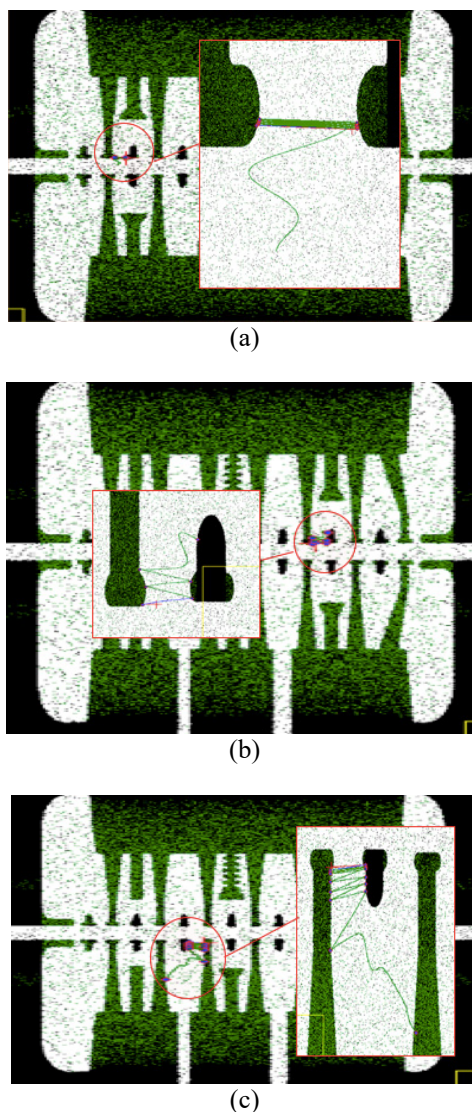


Figure 7: Example of the multipactor trajectories at a different initial level voltage: (a) $U_N = 0.004$; (b) $U_N = 0.007$; (c) $U_N = 0.01$.

CONCLUSION AND OUTLOOK

Critical regions of multipactor avalanches at different levels of the accelerating voltage are identified. It is shown, that the trajectories in the entire range of accelerating voltages decay, but the decay rate is different. A detailed comparison with experimental results is planned for the future. Data on the location of multipactor trajectories in sc CH structures at different voltage levels will be taken into account for the development of short spoke structures for the HELIAC [14, 15]. This re-buncher cavity has a narrow and long gap and can be used for other projects applying sc cavities [16-22].

REFERENCES

- [1] W. Barth *et al.*, “ U^{28+} -intensity record applying a H₂ gas stripper cell”, *Phys. Rev. ST Accel. Beams* 18, no. 040101, 2015.

- [2] W. Barth *et al.*, “Upgrade program of the high current heavy ion UNILAC as an injector for FAIR”, *Nucl. Instrum. Methods Phys. Res., Sect. A*, vol. 577, no. 211, 2007.
- [3] L. Groening *et al.*, “Benchmarking of measurement and simulation of transverse rms-emittance growth”, *Phys. Rev. ST Accel. Beams* 11, no. 094201, 2008.
- [4] W. Barth *et al.*, “Heavy ion linac as a high current proton beam injector”, *Phys. Rev. ST Accel. Beams* 18, no. 050102, 2015.
- [5] A. Adonin *et al.*, “Beam brilliance investigation of high current ion beams at GSI heavy ion accelerator facility”, *Rev. Sci. Instrum.*, vol. 85, no. 02A727, 2014.
- [6] W. Barth *et al.*, “High brilliance uranium beams for the GSI FAIR”, *Phys. Rev. ST Accel. Beams*, vol. 20, no. 050101, 2017.
- [7] W. Barth *et al.*, “A superconducting CW-LINAC for heavy ion acceleration at GSI”, in *Proc. EPJ Web Conf.*, vol. 138, no. 01026, 2017.
- [8] F. Dziuba *et al.*, “First performance test on the superconducting 217 MHz CH cavity at 4.2 K”, in *Proc. LINAC’16*, East Lansing, MI, USA, 2016, pp. 953–955.
- [9] F. Dziuba *et al.*, “First cold tests of the superconducting cw demonstrator at GSI”, in *Proc. RuPAC’16*, St. Petersburg, Russia, paper WECBMH01, 2016.
- [10] W. Barth *et al.*, “First heavy ion beam tests with a superconducting multigap CH cavity”, *Phys. Rev. ST Accel. Beams*, vol. 21, no. 020102, 2018.
- [11] Gusarova, M.A., Petrushina, I.I., Khudyakov *et al.*, “New possibilities of MultP-M code”, in *Proc. IPAC’14*, Dresden, Germany, Jun. 2014, pp. 433-435.
- [12] <https://www.cst.com/>.
- [13] R. Calder *et al.*, *Nuclear Instrumentation Methods Physics Res. B, Beam Interaction Matter.*, At., vo. 13, no. 631, 1986.
- [14] M. Gusarova *et al.*, “Design of the two-gap superconducting re-buncher”, in *Proc. IPAC’18*, Vancouver, Canada, Apr.-May 2018, paper 2678, this conference
- [15] K. Taletskiy *et al.*, “Comparative study of low beta multigap superconducting bunchers”, in *Proc. IPAC’18*, Vancouver, Canada, Apr.-May 2018, paper 3364, this conference.
- [16] R. Laxdal, “Recent progress in the superconducting RF Program at TRIUMF/ISAC”, *Physica (Amster-dam)*, vol.441C, no. 13, 2006.
- [17] A. E. Aksent'ev *et al.*, “Conceptual Development of a 600–1000 MeV Proton Beam Accelerator-Driver with Average Beam Power >1 MW”, *Atomic Energy*, vol. 117, no. 4, pp 270–277, 2015.
- [18] K. A. Aliev *et al.*, “On application of superconducting resonators for reconstruction of proton injector for nuclotron complex”, *Physics of Particles and Nuclei Letters*, vol.13, no. 7, Dec. 2016, pp. 911-914.
- [19] Aliev, K.A. *et al.*, “Study of superconducting accelerating structures for megawatt proton driver linac”, in *Proc. 24th Russian Particle Accelerator Conference*, Obninsk, Russian Federation, Oct. 2014, pp. 318-320.
- [20] Gusarova, M.A. *et al.*, “Research and design of a new RFQ injector for modernization of the LU-20 drift-tube linac”, *Physics of Particles and Nuclei Letters*, vol. 13, no. 7, Dec. 2016, pp. 915-918.
- [21] N. Solyak *et al.*, “The concept design of the CW linac of the Project X”, in *Proc. IPAC’10*, Kyoto, Japan, 2010, pp. 654–656.
- [22] A. V. Butenko *et al.*, “Development of NICA injection complex”, in *Proc. IPAC’14*, Dresden, Germany, Jun. 2014, pp. 2103–2105.